Applied Physics Research; Vol. 16, No. 1; 2024
ISSN 1916-9639 E-ISSN 1916-9647
Published by Canadian Center of Science and Education

Variability of the Magnetospheric Convection Electric Field (MCEF) Under Shock Activity During the Solar Cycle 24

Nongobsom BAZIE[1], Christian ZOUNDI[1], Alfred Jean Stéphane DAMA[1] & Frédéric OUATTARA[1]

[1] Laboratoire de Chimie Analytique, de Physique Spatiale et Energétique (L@CAPSE), Université Norbert ZONGO, Koudougou, Burkina Faso

Correspondence: Christian ZOUNDI, Laboratoire de Chimie Analytique, de Physique Spatiale et Energétique (L@CAPSE), Université Norbert ZONGO, Koudougou, Burkina Faso.

Received: February 17, 2024 Accepted: March 19, 2024 Online Published: April 8, 2024

doi:10.5539/apr.v16n1p134 URL: https://doi.org/10.5539/apr.v16n1p134

Abstract

In the present work, we have analyzed the statistical variability of the MCEF under shock activity during solar cycle 24 as a function of the different phases of solar cycle 24 and as a function of the seasons. We compared the MCEF under shock periods with that under quiet periods. Solar cycle 24 recorded an average MCEF value of 0.28816888 mV/m, i.e. an average value of 0.26399935 mV/m for the ascending phase, 0.2961038 mV/m for the maximum phase and 0.28652747 mV/m for the descending phase. The minimum quantitative deviation from quiet activity observed is 59%. Seasonally, the highest MCEF values were recorded in Summer and Winter, and the lowest in Autumn and Spring. The corresponding mean values are 0.32707785 mV/m, 0.30966472 mV/m, 0.27061512 mV/m and 0.27020401 mV/m respectively. The minimum quantitative deviation from quiet activity observed is 66 %. This study showed that in most cases magnetic reconnection occurs on the night side between 1800 UT and 2400 UT.

Keywords: magnetospheric convection electric field, shock activity, magnetic reconnection, coronal mass ejections, solar cycle phases

1. Introduction

During the interaction between the solar wind and the magnetosphere, a huge amount of solar plasma is transmitted to the magnetosphere through various solar activities such as solar flares (SF), coronal mass ejections (CMEs) and corotating interaction regions (CIRs) During the interaction between the solar wind and the magnetosphere, a huge amount of solar plasma is transmitted to the magnetosphere through various solar activities such as solar flares (SF), coronal mass ejections (CMEs) and corotating interaction regions (CIRs) (Cane, 2000; Gautam et al., 2022; Parker, 1958; Silwal et al., 2021; Subedi et al., 2017; Tsurutani et al., 1992). The movement of plasma in the magnetosphere is governed by an electric field resulting from the interaction between the solar wind and the magnetosphere. This electric field, responsible for magnetospheric convection, is oriented from dawn to dusk (Axford, 1969; Vasyliunas, 1970; Chappell, 1974; Stern, 1975). Several studies (Dungey, 1961, 1963; Carpenter, 1967; Rycroft & Thomas, 1970; Lei et al., 1981; Revah & Bauer, 1982; Bothmer et al., 2007; Kacem et al., 2018; Marchaudon, 2018; Salfo & Frédéric, 2018) have been carried out to understand magnetospheric dynamics and the MCEF's dependence on geomagnetic activity and solar wind parameters. Shock activity occurs on days with sudden storm commencement (SSC) when the geomagnetic index $Aa \geq 20$ nT (Legrand & Simon, 1989; Mayaud, 1973; Ouattara & Amory-Mazaudier, 2009; Zerbo et al., 2012) Shock activity is caused by coronal mass ejections (CMEs).

Today, the magnetic reconnection proposed by Dungey (1961) is accepted as the main mechanism by which energy and matter are transferred to the magnetosphere.

Previous studies have also highlighted the dependence of: (1) the MCEF on geomagnetic activity (Carpenter, 1967; Rycroft & Thomas, 1970; Salfo & Frédéric, 2018), (2) the MCEF on the orientation of the interplanetary magnetic field (IMF) (Bothmer et al., 2007; Kacem et al., 2018; Marchaudon, 2018) and (3) the MCEF on the interplanetary electric field (IEF) of the solar wind (Lei et al., 1981; Revah & Bauer, 1982).

The studies carried out by Salfo et Frédéric (2018) and DAMA et al. (2023) did not take into account seasonal fluctuations in MCEF. Also, according to Marchaudon (2018), the MCEF varies in intensity according to the efficiency of the magnetic reconnection process and in direction according to the orientation of the interplanetary magnetic field (IMF). As the hourly values of the MCEF are algebraic values (positive and negative), summation to obtain hourly averages can cancel out the MCEF and cancel out or reduce the impact of solar activity on the MCEF. As a result, the MCEF's hourly E intensities need to be taken into account for the statistical study.

In this work, we analyse the statistical variability of the MCEF under shock activity as a function of the different phases of solar cycle 24 and as a function of the seasons, by taking into account its intensity E.

In Section 2, the data and methodology of the study are presented. The results and discussions are presented in Section 3, and the conclusion is given in Section 4.

2. Data and Methodology

2.1 Data

The E_y values of the IEF frozen in the solar wind are used to determine the MCEF. They are available at https://omniweb.gsfc.nasa.gov/form/dx1.html.

2.2 Methodology

Quiet days are characterised by an aa index of less than 20 nT. Shock activity days are SSC days where the aa index remains greater than or equal to 20 nT for one, two or three days. In order to ensure that they were indeed the consequences of shock events (CMEs), we took into account the restriction criterion proposed by BAZIE et al.(2023). A total of fifty-two (52) SSC shocks were selected for the study.

MCEF values are obtained using the linear correlation between hourly Ey and MCEF data established by Lei et al.(1981) and validated by Revah and Bauer (1982) (equation (1)). In our study, we take into account the intensity E of the MCEF (equation (2)).

$$MCEF = 0.13\, E_y + 0.09 \quad (1)$$

$$E = |MCEF| \quad (2)$$

We used the formulas given in equations (3) and (4) to calculate the hourly average values of the intensity E of the MCEF.

In these equations, E_{hm} denotes the monthly hourly average value of E, n_m the number of months, E_{hj} the daily hourly average value of E, n_{jd} the number of days of available data and $E_{activity}$ the hourly average value of E during the activity in question.

$$E_{activity} = \frac{\sum E_{hm}}{n_m} \quad (3)$$

$$E_{hm} = \frac{\sum E_{hj}}{n_{jd}} \quad (4)$$

For the seasonal study, we have adopted the following division: Winter (December-January-February), Spring (March-April-May), Summer (June-July-August) and Autumn (September-October-November). The solar cycle is divided into phases as follows: minimum phase (2008-2009), ascending phase (2010-2011), maximum phase (2012-2014) and descending phase (2015-2018). No SSC shock was observed during the minimum phase of the solar cycle, so it is not taken into account in our study.

Error bars are placed on the quiet activity graph in order to qualitatively analyze the two (02) graphs. The relative deviations or quantitative differences Δ of the MCEF for the period of shock activity compared to the quiet activity period, expressed as a percentage, are obtained by equation (5).

$$\Delta = \frac{E_{Shock} - E_{Quiet}}{E_{Shock}} \times 100 \quad (5)$$

3. Results and Discussion

3.1 Diurnal Variations of MCEF During Solar Cycle Phases

Figure **1** shows the diurnal variations of the MCEF under shock activity, without distinction of CMEs type, and under quiet activity during solar cycle 24. The red graphs show the diurnal evolution of the MCEF during the disturbed period, while the blue graphs show the diurnal evolution of the MCEF during the quiet period. Panels (a), (b), (c) and (d) correspond respectively to the diurnal variations of the MCEF of the ascending phase, the maximum phase and the descending phase.

In all the panels, the graph of shock activity is above that of quiet activity. This could reflect the impact of shock activities on the MCEF during cycle 24 and its various phases. Furthermore, in panels **(a)** and **(c)**, the shock activity graph shows a general decreasing trend from 0000 UT to 1800 UT and a general increasing trend from 1800 UT to 2400 UT. Panel **(b)** shows a general decreasing trend from 0000 UT to 0500 UT and from 1800 UT to 2400 UT, and an increasing trend from 0500 UT to 1800 UT. In panel **(d),** the general trend of the graph is increasing between 0000 UT and 0500 UT and between 1800 UT and 2400 UT, between 0500 UT and 1800 UT, the general trend of the curve is decreasing.

MCEF variability during quiet periods shows a generally monotonous trend. This variability is attributed to a lack of reconnection between interplanetary magnetic field lines and geomagnetic field lines (McPherron et al., 2008; Salfo & Frédéric, 2018). The increasing and decreasing phases observed in the daily evolution of the MCEF respectively reflect the increase and decrease in convection following the amplification or decrease in intensity of the shock activity (Salfo & Frédéric, 2018). The intensity of the MCEF varies with the efficiency of the magnetic reconnection process, according to Marchaudon (2018). As a result, the MCEF's increasing phase is attributed to the reconnection between the IMF lines and those of the geomagnetic field. Similarly, the decreasing phase is attributed to a weakening or cessation of the magnetic reconnection process. For Dungey (1961) and Dungey (1963), magnetic reconnection occurs efficiently when the IMF has a southerly orientation. The increasing phase of the MCEF then corresponds to the IMF's southward orientation, and the decreasing phase corresponds to the IMF's northward orientation. The observed change in trend corresponds to the inversion of the IMF. Magnetic reconnection seems plausible at night between 1800 UT and 2400 UT except during the ascending phase when it would occur on the day side between 0500 UT and 1200 UT.

The minimum MCEF values recorded are 0.2598623 mV/m at 1600 UT during the solar cycle, 0.15458444 mV/m at 0300 UT during the ascending phase, 0.25920625 mV at 1400 UT during the maximum phase and 0.24636085 mV/m at 1800 UT during the descending phase. For maximum values, we recorded 0.35125203 mV/m at 2300 UT during the solar cycle, 0.406845 mV/m at 1200 UT for the ascending phase, 0.35422847 mV/m at 1900 UT for the maximum phase and 0.35803857 at 2300 UT for the descending phase. On average, we obtain an MCEF value of 0.28816888 mV/m for the solar cycle, 0.26399935 mV/m for the ascending phase, 0.2961038 mV/m for the maximum phase and 0.28652747 mV/m for the descending phase.

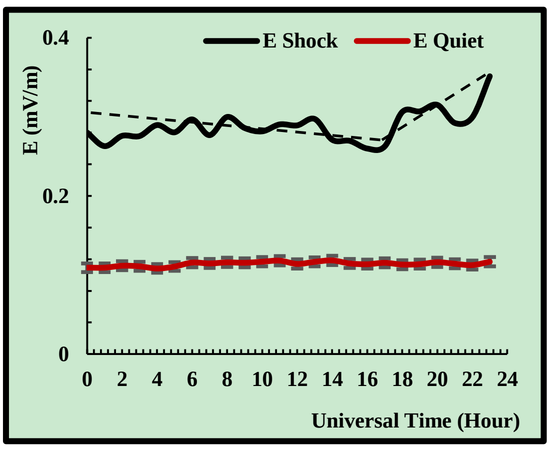

(a) Solar cycle 24

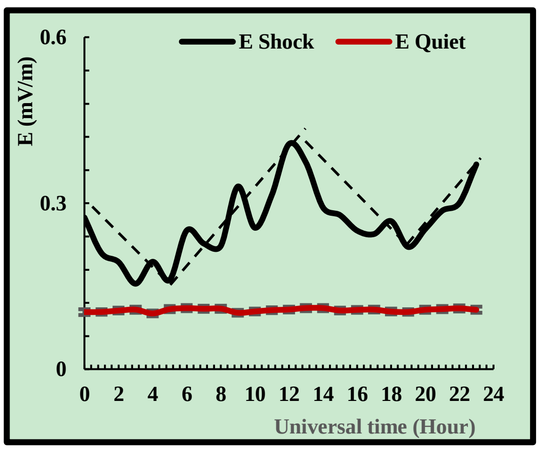

(b) Ascending phase

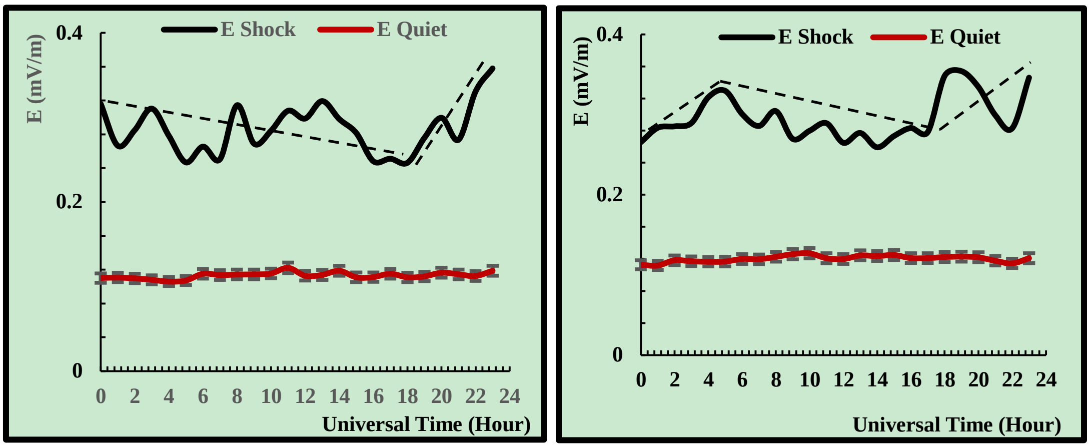

(c) Descending phase (d) Maximum phase

Figure 1. Diurnal variations of MCEF during solar cycle phases

Table 1 gives the quantitative deviations Δ of the MCEF for the disturbed period compared to the reference quiet period. The minimum gaps are about 56% for the solar cycle, 54% for the descending phase, 52% for the phase maximum and 30% for the ascending phase. These very remarkable differences between the magnetic quiet and the disturbed period can be explained by the amplification of the various magnetospheric currents underpinned by high values of MCEF (Woelfflé, 2010).

Table 1. MCEF quantitative deviations during solar cycle phases

UT **(Hour)**	**Cycle**	**Ascending phase**	**Descending phase**	**Maximum phase**
0	60.9751069	62.29680409	65.153033	57.60190867
1	58.4511713	50.63469424	58.49851996	60.62477673
2	59.5233531	45.31017988	61.5165279	58.56033865
3	59.7441826	30.27781109	65.21832802	59.59504466
4	62.6307889	48.03473969	61.962972	63.82071552
5	60.5193911	32.72771221	56.58949975	64.62647414
6	61.0082384	55.96634757	56.63700409	60.12766462
7	58.5939516	51.86116586	54.69358193	58.18274457
8	61.3201152	50.8237281	63.68390837	59.74583743
9	59.607183	69.06553387	57.45702753	53.32766898
10	58.5245089	59.14712471	59.40858902	54.65002944
11	59.3229844	66.0917878	60.32685269	58.25206111
12	60.5752792	73.46369768	62.26011705	54.76808091
13	60.7590077	70.35670338	64.37068587	55.16211939
14	56.2978701	62.16068735	60.18274283	52.35691741
15	57.4935542	61.85520401	60.59171929	54.35192222
16	56.2758317	57.17452119	55.2159385	57.29957929
17	56.0423047	55.88525597	54.11930055	56.53378762
18	63.0216186	61.09271905	54.98249508	64.88403662
19	62.9572475	53.12820287	59.42222388	65.31372327
20	63.1319079	57.52527592	61.14395738	63.5553056
21	60.9143468	62.01371405	58.14819672	60.71112246
22	62.3947567	63.33077578	65.98115316	59.59087608
23	66.7544883	70.96660601	66.85289467	65.09204253

This increase of the MCEF intensity during shock activity corroborates the observation made by Hanuise et al. (2006) that there is an increase in the density of particles in the E region during a coronal mass ejection. As a result, ionosphere-magnetosphere coupling leads to the precipitation of energetic particles into the magnetosphere, increasing the intensity of the MCEF. The maximum deviations are about 67% for the solar cycle and the descending phase, 73% for the ascending phase, 65% for the maximum phase. The behavior of the MCEF during the maximum and descending phases is similar to that of the MCEF observed on average throughout cycle 24. This could be explained by the high number of geoeffective CMEs during the maximum and descending phases (BAZIE et al., 2023). The minimum and maximum deviations recorded at the ascending phase suggest that there is no clearly identifiable relationship between MCEF intensity and solar phase. This result corroborates the observations of Woefflé (2010).

3.2 Diurnal Variations of MCEF During Seasons

Figure 2 shows the diurnal and seasonal variations of the MCEF under shock activity, and under quiet activity during solar cycle 24. Panels **(a)**, **(b)**, **(c)**, **(d)** show diurnal variations of the MCEF in Autumn, Summer, Winter and Spring respectively. The black graphs show the diurnal evolution of the MCEF under shock activity, while the red graphs show the diurnal evolution of the MCEF under quiet activity. It can be seen in all panels that the shock activity graph is completely above the quiet activity graph. This shows that over the four (04) seasons, shock activities have had a significant impact on the MCEF.

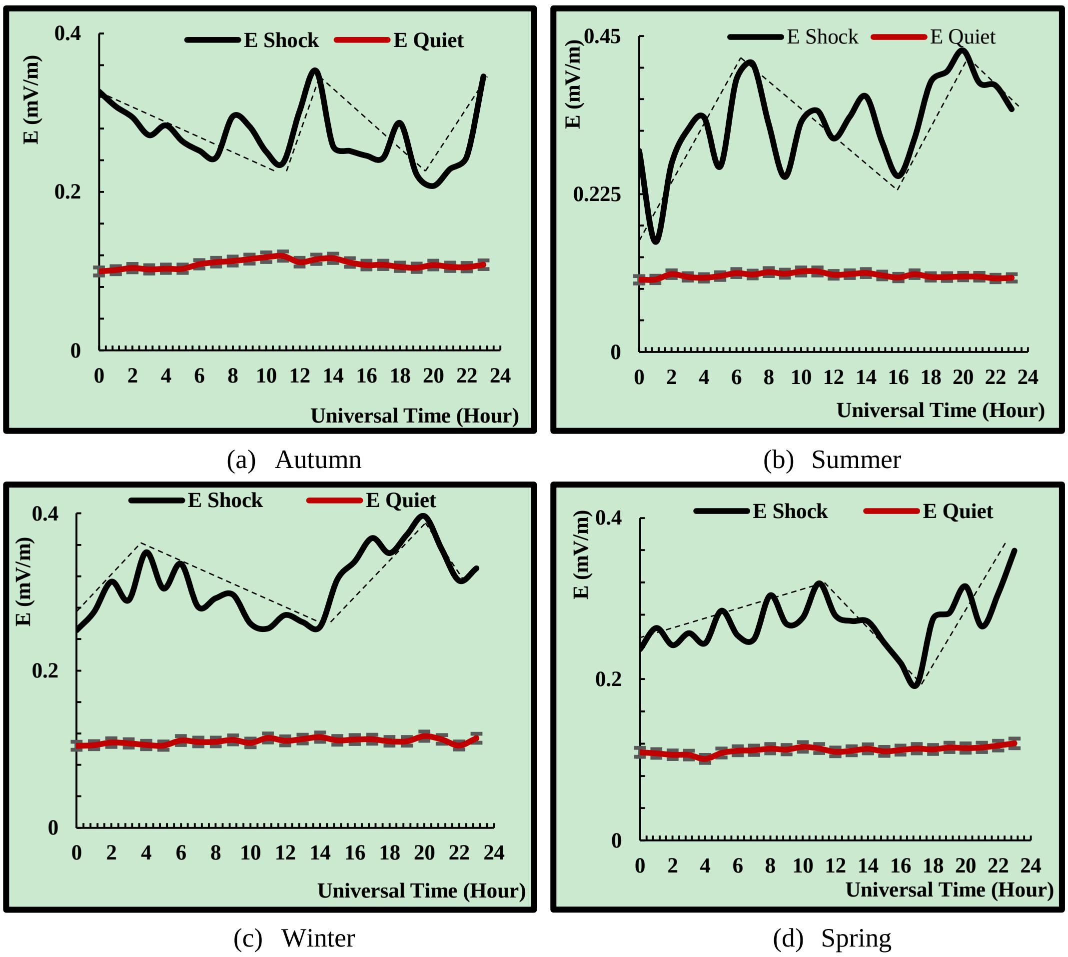

Figure 2. Diurnal variations of MCEF during seasons

Panel **(a)** shows that the MCEF decreases from 0000 UT to 1100 UT and 1300 UT to 2000 UT, in Autumn. This decrease of the MCEF reflects a drop in the level of shock activity and therefore a weakening or cessation of the magnetic reconnection process during these periods. Between 1000 UT and 1300 UT, the MCEF rises sharply, reaching a maximum value of 0.35241611 mV/m at 1300 UT. This period corresponds to a reconnection that occurs on the day side following a southward orientation of the IMF according to Dungey (1961). Between 2000 UT and 2400 UT, there is a night-time reconnection.

In summer (panel **(b)),** the morning and evening sides are reconnected, with the MCEF increasing between 0000 UT and 0700 UT and between 1600 UT and 2000 UT respectively. Maximum MCEF values are 0.41106204 mV/m at 0700 UT and 0.42957685 mV/m at 2000 UT. In addition, 0700 UT and 2000 UT correspond to times when the IMF was oriented northwards, thus hindering reconnection and reducing the MCEF.

In panel **(c)**, the MCEF increases from 0000 UT to 0400 UT and 1400 UT to 2000 UT. This increase of the MCEF indicates the intensification of the magnetic reconnection process in Winter. The maximum MCEF values are 0.3505254 mV/m at 0400 UT and 0.39666349 mV/m at 2000 UT. Between 0400 UT and 1400 UT, 2000 UT and 2400 UT, the MCEF decreases. These periods correspond to the decrease or cessation of the reconnection process occurring on the day side due to the change in direction of the IMF towards the north. Between 2000 UT and 2400 UT, there is a nocturnal reconnection.

In spring, reconnection occurs on the day side from 0000 UT to 1100 UT and on the night side from 1600 UT to 2400 UT. This reconnection is supported by the increase of the MCEF during these periods. The maximum MCEF values recorded during these increasing phases were 0.31891004 mV/m at 1100 UT and 0.35939825 mV/m at 2400 UT.

The minimum MCEF values recorded are 0.20743222 mV/m at 2000 UT in Autumn, 0.15680185 mV/m at 0100 UT in Summer, 0.25126845 mV/m at 0100 UT in Winter and 0.19313675 mV at 1700 UT in Spring. The maximum values obtained are respectively 0.35241611 mV/m at 1300 UT, 0.35939825 mV/m at 2400 UT, 0.39666349 mV/m at 2000 UT, 0.42957685 mV/m at 2000 UT, in Autumn, Spring, Winter and Summer. On average, the MCEF values recorded during Spring, Autumn, Winter and Summer respectively, in ascending order, were 0.27020401 mV/m, 0.27061512 mV/m, 0.30966472 mV/m and 0.32707785 mV/m.

The quantitative deviations Δ of the MCEF for the disturbed period compared with the quiet period taken as a reference, are given in Table 2. Minimum deviations are about 48 % in Autumn, 34 % in Summer, 56 % in Winter and 41 % in Spring. Maximum deviations are about 69 % in Autumn, 75 % in Summer, 71 % in Winter and 66 % in Spring.

Table 2. Quantitative deviations of MCEF during seasons

UT (Hour)	Autumn	Summer	Winter	Spring
0	69.4931272	64.0639981	58.5112468	53.9575767
1	67.0633787	34.2009966	61.7133858	59.0170087
2	64.644856	58.708871	65.3657647	56.1586789
3	62.3495914	66.2499053	62.8879783	58.7815401
4	63.7186984	68.3834849	69.9191623	58.6903193
5	60.9445922	59.0333287	65.6373798	61.9492904
6	56.8669746	71.0346486	66.9401244	56.2408463
7	54.2467048	73.1784344	61.1270992	55.2238698
8	61.805443	64.9567819	62.5625168	62.5628991
9	59.2497971	55.2829249	62.2989584	58.0039419
10	53.0918746	64.9602485	58.4449053	58.0335533
11	49.6105745	66.5890597	54.9152337	64.2464441
12	63.1669801	63.8386781	59.1189557	60.6125499
13	67.3908929	66.8930166	56.8667119	59.1305097
14	54.9103361	69.1098966	54.8742038	58.1337121
15	55.9139893	63.5175591	64.8229048	54.9433541
16	56.1826158	57.6628311	66.8748797	49.1073227

17	55.5687707	63.5825038	69.4424433	41.0168803
18	63.278314	72.1881455	68.5382159	58.9201648
19	53.0539733	73.2904221	70.4930646	59.1385219
20	48.1148318	74.9954279	70.6186292	63.6908372
21	53.9570683	72.0452538	68.2726718	56.5646174
22	57.0272915	72.3807599	66.7018312	61.5546015
23	68.7201976	69.4325219	65.4633309	66.4863231

4. Conclusion

Our study confirms the influence of shock activity on the MCEF according to the phases of solar cycle 24 and the seasons. On average, solar cycle 24 recorded an MCEF value of 0.28816888 mV/m, i.e. an average value of 0.26399935 mV/m for the ascending phase, 0.2961038 mV/m for the maximum phase and 0.28652747 mV/m for the descending phase.

The seasonal study revealed that MCEF values are highest in Summer and Winter. Low values are obtained in Autumn and Spring. The corresponding mean values are, respectively, 0.27020401 mV/m, 0.27061512 mV/m, 0.30966472 mV/m and 0.32707785 mV/m. The diurnal evolution of the MCEF is sometimes increasing, sometimes decreasing. The increasing and decreasing phases reflect the dynamics of the reconnection process between the interplanetary magnetic field lines and those of the geomagnetic field.

Overall, this study was of interest to understand the variability of the MCEF during periods of shock activity during solar cycle 24, depending on solar phases and seasons. However, it does not allow us to understand the dynamics of the MCEF during isolated geoffective coronal mass ejections. In another study, we propose to analyse the variability of the MCEF during magnetic disturbances generated by coronal mass ejections.

We can also provide summary statistics, such as mean, median, standard deviation and variance for MCEF values. This will be an opportunity for discussion of the trends observed in the data and their implications.

Acknowledgments

The authors thank OMNIWEB team for the E_y values of the IEF frozen in the solar wind.

Authors' contributions

Dr Christian ZOUNDI, Mrs Nongobsom BAZIE and Alfred Jean Stéphane DAMA (two doctoral students), were responsible for data collection and study design. Dr. Christian ZOUNDI and Mrs Nongobsom BAZIE drafted the manuscript and Prof. Frédéric OUATTARA revised it. All authors read and approved the final manuscript.

Funding

This work was supported by the contribution of the authors.

Competing interests

The authors declare that they have no known competing financial interests or personal relationships that could have appeared to influence the work reported in this paper.

Informed consent

Obtained.

Ethics approval

The Publication Ethics Committee of the Canadian Center of Science and Education.

The journal and publisher adhere to the Core Practices established by the Committee on Publication Ethics (COPE).

Provenance and peer review

Not commissioned; externally double-blind peer reviewed.

Data availability statement

The data that support the findings of this study are available on request from the corresponding author. The data are not publicly available due to privacy or ethical restrictions.

Data sharing statement

No additional data are available.

Open access

Copyrights

References

Axford, W. I. (1969). Magnetospheric convection. *Reviews of Geophysics*, *7*(1-2), 421-459.

Bazie, N., Zoundi, C., Dama, A. J. S., & Ouattara, F. (2023). Corrélation entre le nombre de taches solaires (Rz) et les événements de chocs au cours du cycle solaire 24. *Revue burkinabè de la recherche Science et Technique*, *42*(1), 327-343.

Bothmer, V., Daglis, I. A., & Russell, C. T. (2007). The coupling of the solar wind to the Earth's magnetosphere. *Space weather-physics and effects*, 103-130.

Cane, H. V. (2000). Coronal mass ejections and Forbush decreases. *Space Science Reviews*, *93*(1-2), 55-77.

Carpenter, D. L. (1967). Relations between the dawn minimum in the equatorial radius of the plasmapause and Dst, Kp, and local K at Byrd Station. *Journal of Geophysical Research*, *72*(11), 2969-2971.

Chappell, C. R. (1974). Detached plasma regions in the magnetosphere. *Journal of Geophysical Research*, *79*(13), 1861-1870.

Dungey, J. W. (1961). Interplanetary magnetic field and the auroral zones. *Physical Review Letters*, *6*(2), 47.

Dungey, J. W. (1963). Interactions of solar plasma with the geomagnetic field. *Planetary and Space Science*, *10*, 233-237.

Gautam, S. P., Silwal, A., Poudel, P., Karki, M., Adhikari, B., & Chapagain, N. P. (2022). Study of Solar Wind and Interplanetary Magnetic Field Features Associated with Geomagnetic Storms : The Cross Wavelet Approach. *Authorea Preprints*.

Hanuise, C., Cerisier, J.-C., Auchère, F., Bocchialini, K., Bruinsma, S., Cornilleau-Wehrlin, N., Jakowski, N., ... Valette, J.-J. (2006). From the Sun to the Earth: Impact of the 27-28 May 2003 solar events on the magnetosphere, ionosphere and thermosphere. *Annales Geophysicae*, *24*(1), 129-151.

Kacem, I., Jacquey, C., Génot, V., Lavraud, B., Vernisse, Y., Marchaudon, A., ... Hasegawa, H. (2018). Magnetic reconnection at a thin current sheet separating two interlaced flux tubes at the Earth's magnetopause. *Journal of Geophysical Research: Space Physics*, *123*(3), 1779-1793.

Legrand, J., & Simon, P. (1989). Solar cycle and geomagnetic activity: A review for geophysicists. Part I. The contributions to geomagnetic activity. *Ann. Geophys*, *7*, 565-578.

Lei, W., Gendrin, R., Higel, B., & Berchem, J. (1981). Relationships between the solar wind electric field and the magnetospheric convection electric field. *Geophysical Research Letters*, *8*(10), 1099-1102.

Marchaudon, A. (2018). *Observation et modélisation des processus de couplage entre la magnétosphère et l'ionosphère terrestres*. Université Paul Sabatier, Toulouse.

Mayaud, P.-N. (1973). A hundred year series of geomagnetic data, 1868-1967, indices aa, storm sudden commencements. *IAGA Bulletin, No. 33*.

McPherron, R. L., Weygand, J. M., & Hsu, T.-S. (2008). Response of the Earth's magnetosphere to changes in the solar wind. *Journal of Atmospheric and Solar-Terrestrial Physics*, *70*(2-4), 303-315.

Ouattara, F., & Amory-Mazaudier, C. (2009). Solar–geomagnetic activity and Aa indices toward a standard classification. *Journal of Atmospheric and Solar-Terrestrial Physics, 71*(17-18), 1736-1748.

Parker, E. N. (1958). Dynamics of the interplanetary gas and magnetic fields. *Astrophysical Journal, 128*, 664.

Revah, I., & Bauer, P. (1982). Rapport d'activité du Centre de Recherches en Physique de l'environnement Terrestre et Planétaire. *Note technique CRPE/115*, 38-40.

Rycroft, M. J., & Thomas, J. O. (1970). The magnetospheric plasmapause and the electron density trough at the Alouette I orbit. *Planetary and Space Science*, *18*(1), 65-80.

Salfo, K., & Frédéric, O. (2018). *Magnetosphere convection electric field (MCEF) time variation from 1964 to 2009: Investigation on the signatures of the geoeffectiveness coronal mass ejections*.

Silwal, P., Kim, J. K., Jeon, S. M., Lee, J.-Y., Kim, Y. J., Kim, Y. S., … Lee, M. J. (2021). Mitofusin-2 boosts innate immunity through the maintenance of aerobic glycolysis and activation of xenophagy in mice. *Communications biology*, *4*(1), 548.

Stéphane, D. A., Salfo, K., Alphonse, S. S., & Frédéric, O. (2023). *Variability of the electric field of magnetospheric convection in recurrent activity during the solar cycle 24*.

Stern, D. P. (1975). Quantitative models of magnetic and electric fields in the magnetosphere. *Tropical Conf. on Quantitative Magnetospheric Models*, *X-602-75-90*.

Subedi, L., Lee, T. H., Wahedi, H. M., Baek, S.-H., & Kim, S. Y. (2017). Resveratrol-enriched rice attenuates UVB-ROS-induced skin aging via downregulation of inflammatory cascades. *Oxidative Medicine and Cellular Longevity*.

Tsurutani, B. T., Gonzalez, W. D., Tang, F., & Lee, Y. T. (1992). Great magnetic storms. *Geophysical Research Letters*, *19*(1), 73-76.

Vasyliunas, V. M. (1970). Mathematical models of magnetospheric convection and its coupling to the ionosphere. *Particles and Fields in the Magnetosphere: Proceedings of a Symposium Organized by the Summer Advanced Study Institute, Held at the University of California, Santa Barbara, Calif., August 4–15, 1969*, 60-71.

Woelfflé, A. (2010). *Étude et modélisation du transport de plasma dans la magnétosphère interne*. Toulouse, ISAE.

Zerbo, J. L., Amory Mazaudier, C., Ouattara, F., & Richardson, J. D. (2012). Solar wind and geomagnetism : Toward a standard classification of geomagnetic activity from 1868 to 2009. *Annales Geophysicae*, *30*(2), 421-426.